J. Phys. Chem. A 2002, 106, 10843−10848

Femtosecond Photodissociation Dynamics of Excited-State SO_2[†]

Eric S. Wisniewski[‡] **and A. Welford Castleman, Jr.***[‡,§]

Departments of Chemistry and Physics, The Pennsylvania State University, University Park, Pennsylvania 16802

Received: February 26, 2002

Photodissociation dynamics of SO_2 were investigated employing a multiphoton pump−probe excitation technique (312 nm pump/624 nm probe), with evidence supporting the processes being initiated through the $\tilde{E}$ state. The pump−probe optical transient for the SO_2 species was fit to a single-exponential decay, yielding a time of 271 ± 8 fs. Subsequent decay products of SO and S were also investigated and mathematically fit to determine formation and/or decay time dynamics.

Introduction

In view of its ubiquitous nature, interest in the photochemistry of sulfur dioxide (SO_2) is wide ranging. SO_2 is produced in an industrial setting mainly (∼98%) for use as a precursor to sulfuric acid (H_2SO_4).[1] In this context, it is produced by the combustion of elemental sulfur or by the oxidation of sulfides. However, it is the unintentional production of sulfur oxides as the byproduct of common combustion of hydrocarbon fuels containing sulfidic sulfur, and its subsequent release into the atmosphere, that is of concern to the scientific community. It has been determined that at least 90% of sulfur present in fossil fuel is released in the gas phase as SO_2 during combustion.[2] It is also present in the atmosphere due to volcanic emissions and through the oxidation of various sulfur-containing gases liberated through biochemical cycles. Because of this fundamental importance to atmospheric science, sulfur oxides have been increasingly researched and their chemistry discussed in the literature.[3−6]

Previous work has been conducted in our laboratory on the chemistry of SO_2 with other species.[4,6−10] Some years ago, studies were undertaken to identify reactions with neutral hydroxyl radicals as being a significant mechanism of its initial chemical conversion in the atmosphere. Subsequently, we initially investigated the reaction of SO_2 with $OH^-(H_2O)_{n=0-2}$ and found the presence of $HSO_3-(H_2O)_m$ in the mass spectral distribution of reaction products.[8] From this, the following reaction was postulated:

$$OH^-(H_2O)_n + SO_2 \rightarrow HSO_3^-(H_2O) + (n - m)(H_2O) \quad (1)$$

Further studies by Yang and Castleman of SO_2 with various hydrated anion clusters yielded clues to the role of SO_2 in atmospheric processes.[9] Hydration of anionic species will enable some reactions to become more endothermic due to the stabilization of the reactant ions. More recently, Zhong et al. investigated the dissociative pathways of sulfur dioxide clusters and mixed water−sulfur dioxide clusters.[4] Zhong found that sulfur dioxide cation clusters have an SO_2^+ ion core solvated by SO_2. Furthermore, $[SO(SO_2)_n]^+$ clusters similarly contained an SO^+ ion core with solvation by SO_2 molecules.

The photodissociation of SO_2 has been investigated for several electronically excited states. At 193 nm, its photodissociation yields SO + O exclusively.[11,12] Kawasaki and Sato investigated SO_2 at 193 nm and, from the angular distribution of the dissociative O atom, concluded that the dissociation into SO + O was predissociative. In particular, they found the distribution to be isotropic, indicating that the lifetime of the dissociation is much longer than a rotational period. In other studies, Katagiri et al. experimentally and theoretically explored the $\tilde{C}$ state dissociation of SO_2. They invoked rotational line broadening to claim that the predissociative lifetime of the SO_2 was on the order of 10−100 ps, though the rate was found to increase exponentially as the energy was increased.[13]

Investigations of SO_2 at higher energies showed that along with SO + O, S + O_2 could become a significant dissociation channel.[14,15] Photolysis at 123.6 nm was performed on SO_2 (in the presence of H_2 to minimize experimental difficulties that did not interfere with photodissociation) to yield both dissociation channels in a plethora of excited-state fragments. Lalo and Vermeil suggested that the dissociation process at 123.6 nm to yield S + O_2 proceeded by a direct mechanism. Other studies by Venkitachalam and Bersohn at 285−311 nm (using two-photon excitation) produced S, O_2, SO, and O as photodissociation products.[16] Effenhauser et al. investigated the two-photon photodissociation of SO_2 at 248 and 308 nm.[17] They reported that excitation with photons at 248 nm produced a myriad of photoproducts that yield mostly SO + O, but also fragmentation pathways leading to S + O_2. Furthermore, Effenhauser et al. reported that two-photon excitation at 308 nm resulted in SO + O, in various states. Two-photon photodissociation at 308 nm also produced S photofragments as a minor pathway. Sato reported two-photon (286−309 nm) photodissociation studies of SO_2 that focused on the production of S photofragments, by detection of S by resonance-enhanced ionization.[18]

Sato et al. also reported that a “three-body” dissociation of SO_2 into S + O + O would require three photons of 308 nm light.[18] Two-photon excitation is possible due to the long-lived $\tilde{B}$ state of SO_2. The three-photon process has not been studied and discussed in the literature. This is most likely due to two-photon dissociation that occurs before a third photon is absorbed in nanosecond excitation sources. The Sato “three-body” dis-

---

[†] Part of the special issue “R. Stephen Berry Festschrift”.

* Corresponding author.

[‡] Department of Chemistry.

[§] Depurtment of Physics.

10.1021/jp020535+ CCC: $22.00

sociation has been simulated with three different models: the simultaneous fragmentation, the sequential fragmentation, and the classical impulsive model.[18] For simultaneous fragmentation, S (^{3}P) and S (^{1}D) obtain 0.27 and 0.17 eV of translation energy, respectively. For the classical impulsive model, S (^{3}P) and S (^{1}D) obtain 0.21 and 0.13 eV, respectively. Sato invoked the data obtained from the simulations to conclude that the S atoms produced by two-photon photodissociation (0.21 eV for S (^{3}P) and 0.09 eV for S (^{1}D)) are in reasonable agreement with a proposed simultaneous photodissociation pathway, though Sato claims the two-photon process is most likely. The sequential photodissociation simulation predicts much larger values for the S photofragment; one scenario yielded a value of 0.65 eV for the S (^{3}P) while others yielded values too low to be compared to the experimentally determined energy.

Herein we report the femtosecond pump−probe dynamics of SO_2 monomer on an excited-state surface and the temporal dynamics deduced from the resulting photodissociation products SO, S, and O. Excitation of SO_2 was achieved by a femtosecond laser system with pump photon bandwidth centered at 312 nm.

Experimental Section

The production of SO_2 was indirectly achieved while first attempting to study a unique inorganic species, *N*-thionylaniline. SO_2 monomer was prepared by the hydration of *N*-thionylaniline. Molecular reaction and subsequent rearrangement of the *N*-thionylaniline resulted in the production of aniline and SO_2 (reaction 2):

$$C_6H_5NSO + H_2O \rightarrow C_6H_7N + SO_2 \qquad (2)$$

The reaction products were entrained in helium with a backing pressure of 20 psig. The helium, along with the entrained vapor and other gaseous species, was expanded into the mass spectrometer through a pulsed nozzle. The molecular beam produced in this fashion was collimated with a skimmer prior to ionization with femtosecond laser pulses, which were directed to intercept clusters in a region between the time-of-flight grids. The time-of-flight mass spectrometer is of the Wiley−McLaren design.[19]

Under typical operating conditions, the potential applied to the first time-of-flight grid is between 4 and 5 kV while the potential applied to the second grid is roughly 3 kV. With the reflecting potential applied to the front of the reflectron, the total flight path for the detected ions is 2 m. The detection scheme employs a pair of microchannel plates coupled to a digital oscilloscope (Agilent Technologies 54820A).

Ionization was achieved with an amplified colliding pulse mode-locked ring dye laser (CPM). In this arrangement, a gain jet containing rhodamine 590 tetrafluoroborate is pumped by a continuous wave Nd:YVO_4 laser (Coherent Verdi V5). Continuous wave lasing from the gain jet is interrupted by a second jet containing the saturable absorber DODCI. Laser pulses on the order of 100 fs are generated at 90 MHz with pulse energies of only ∼200 pJ. Amplification of the laser pulses is achieved in four stages using a six-pass bowtie amplifier and three successive Bethune cells, where the beam is progressively expanded from a 2 mm initial diameter to a final beam diameter of 12 mm. All amplification is achieved by transverse pumping of sulforhodamine 640 by the second harmonic of a 10 Hz Nd:YAG laser (Spectra Physics GCR-4). Recompression is performed using a grating pair (1200 lines/mm) to compensate for group velocity dispersion. The amplified laser pulse is <125 fs in duration (sech^2) determined by autocorrelation, has 1.0−1.5 mJ of energy, and has a wavelength centered at 624 nm.

To acquire 312 nm pulses required for pumping the molecules in the two-color pump−probe experiments reported herein, the fundamental laser beam was focused through a β-barium borate (BBO) crystal to generate second harmonic light. The remaining light that is not converted to ultraviolet (UV) is harvested and used as the probe pulse. The UV light is sent through a delay stage so that the optical path lengths of the pump and probe lasers can be adjusted for temporal overlap. A 40 cm optical lens, placed between the focal points of the pump and probe laser pulses, is used to loosely focus the laser pulses between the acceleration grids of the mass spectrometer. It is important to note that only minimal ion signal is present in the mass spectral distribution when either the pump or probe laser pulses are blocked. Hence, neutral excited-state dynamics are investigated and molecular ion states are not probed in the present experiment.

Results and Discussion

Excited-state SO_2 was prepared by multiphoton absorption of the second harmonic output (312 nm) of the CPM laser system. Photodissociation products of SO, S, and O are exhibited in a typical mass spectrum seen in Figure 1. Due to the mass overlap of S and O_2, mass 32 was determined to be sulfur by analysis of the ^{34}S peak that is evident at approximately 4% of mass 32. Further isotopic analysis reveals the presence of a mass 66 amu corresponding to $^{34}SO_2$ and 50 amu corresponding to ^{34}SO.

Two-body dissociation of the SO_2 following excitation to an excited-state yields two major pathways, with a variety of excited and ground-state products:

$$SO_2 \xrightarrow{2h\nu} SO + O \qquad (3)$$

$$SO_2 \xrightarrow{2h\nu} S + O_2 \qquad (4)$$

If both eqs 3 and 4 were operative within the time window of the experiments discussed here, SO_2 would decay via two or more distinct rates. Furthermore, if SO_2 absorbed three pump photons to undergo either a concerted or a stepwise photodissociation mechanism into S + O + O, the kinetics corresponding to this process also would be expected to be revealed in the dynamics of the SO_2 optical transient. Figure 2 displays the pump−probe transient for SO_2. The transient was well fit mathematically to a single-exponential decay, yielding a time of 271 ± 8 fs. The fitting procedure is outlined elsewhere.[20] Attempts were made to mathematically fit the data to single, bi-, and triexponential decay functions; however, the fitting for the bi- and triexponential decay failed to converge. This evidence for a single decay rate for SO_2 is suggestive that only a single decay channel is contributing to the products in these studies.

Figure 3 illustrates the pump−probe transient for SO. Clearly, the production of SO involves a mechanism corresponding to eq 3 but this does not explain the appearance of S, nor the apparent dynamics exhibited by this species which is displayed by the data plotted in Figure 4. If the production of S is due to eq 4, while the dynamics in Figure 3 are explained by eq 3, then the dynamics exhibited in Figure 2 would be expected to be best fit to a biexponential decay since two separate processes would be occurring that decay into two distinct rates. Since this

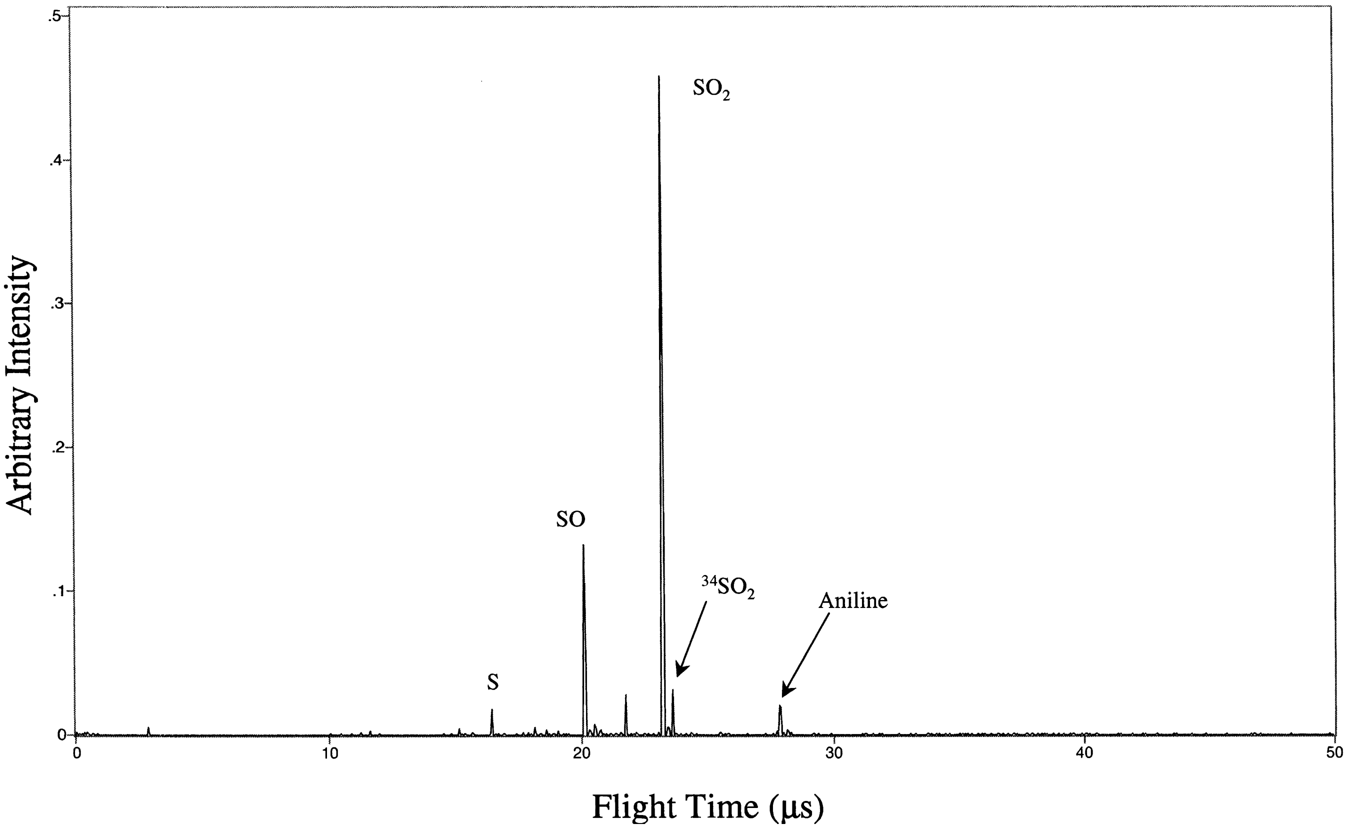

Figure 1. Mass spectrum of SO_2 taken at zero delay between pump and probe laser beams.

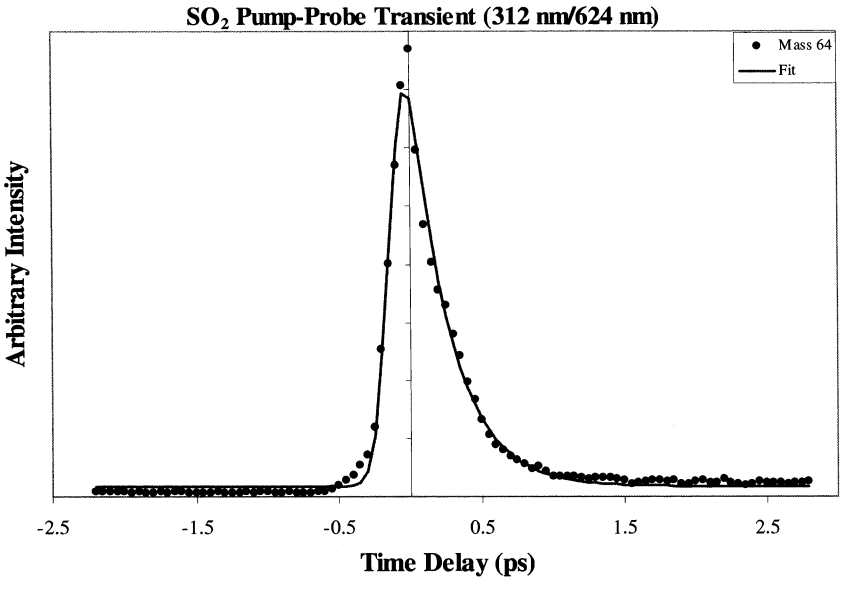

Figure 2. Pump−probe transient for the sulfur dioxide. The data was fit to a single-exponential decay, with deconvolution of the laser pulse width, to yield a time constant of 271 fs.

is not the case, the production of S appears to be due to a secondary fragmentation of SO. The kinetics of the various processes for SO are outlined below:

$$SO_2 \xrightarrow{k_1} f(SO + O) \qquad (5)$$

$$(1 - f)SO \rightarrow S + O \qquad (6)$$

The initial excitation of SO_2 leads to the formation of SO. After the initial production of SO by the decay of SO_2, the ensuing dynamics on the sulfur monoxide are unclear. Several processes may be occurring as discussed in what follows.

First, consider the possibility that sulfur dioxide absorbs two photons to generate the excited $\tilde{E}$ state of SO_2. Following this excitation, photodissociation results to form SO + O. In this mechanism, only those SO molecules with appreciable internal energy (electronically excited) will absorb enough probe photons to become ionized and be imaged; ground-state SO (IP = 10.360 eV) would require six probe photons for ionization. However, the decay dynamics for SO in this mechanism are unaccounted for. Furthermore, the apparent dynamics on the sulfur photofragment also remain unexplained.

A second possible scenario is that the sulfur dioxide may absorb three pump photons and decay into S + O + O. If this

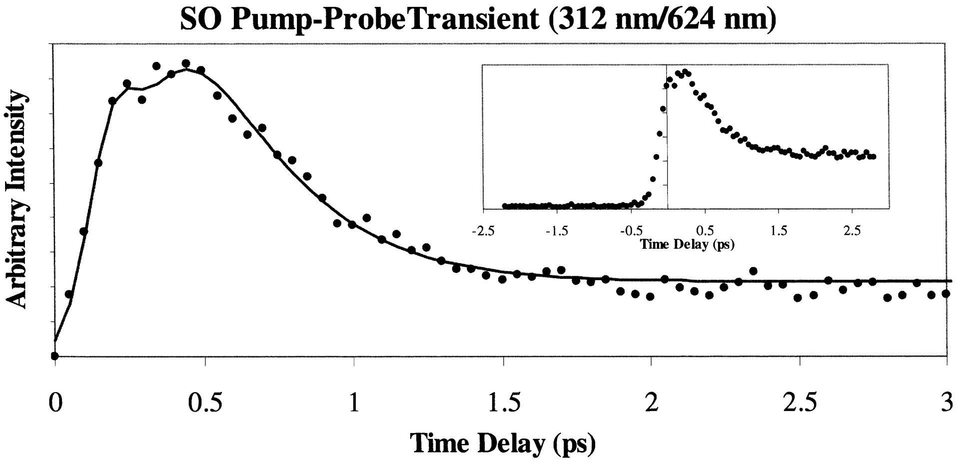

Figure 3. Pump−probe transient for the sulfur monoxide photofragment. The data was fit to kinetic rate equations, with deconvolution of the laser pulse width, to yield a formation time of 271 fs and a decay time of 156 fs. The inset figure is the original SO data, unshifted along the time axis.

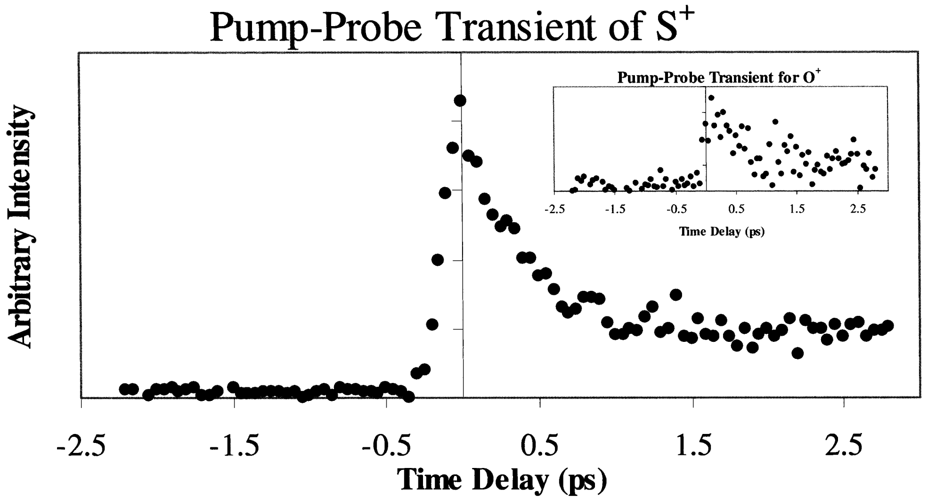

Figure 4. Potential energy surface of SO_2 illustrating the intermediate B state that is accessed in a two-photon absorption scheme.

mechanism was operative, the dissociation must occur in a stepwise fashion so sulfur monoxide is first formed and then decayed. This mechanism fails to account for the SO ion signal that remains at longer delay times. Further experiments to attenuate the pump photon density failed to yield dissociative information suggesting that only two-photon excitation is occurring, and three-photon pumping is negligent. On this basis, excitation via a two-photon absorption scheme through the $\tilde{E}$ state is surmised.

Finally, SO_2 may be absorbing two photons to reach the $\tilde{E}$ state, see Figure 5. Dissociation may then result in SO + O as before, but the sulfur optical transient arises due to the post-ionization fragmentation of SO^+. This explains the dynamics attributed to the sulfur photofragment but fails to fully explain the decay dynamics on the SO fragment. Effenhauser noted that the formation of SO (b $^1\Sigma^+$) is possible by analysis of the photodissociation energetics and noted that a minor contribution of this excited-state cannot be excluded from the data despite the inability to discern whether this state is produced.[17] If SO (b $^1\Sigma^+$), (a $^1\Delta$), and (X $^3\Sigma^-$) were simultaneously produced in the two-photon dissociation of SO_2, it is conceivable that the ionization of each species would behave differently in the mass spectrometer. The ground-state SO may not absorb enough photons for ionization while the SO (a $^1\Delta$), already with ~0.75 eV internal energy, would require one less photon for ionization.[21] However, SO (b $^1\Sigma^+$) may quickly radiatively decay to ground-state sulfur monoxide which would account for the dynamics observed in these experiments. This mechanism may also explain why Effenhauser was unable to discern this excited state.

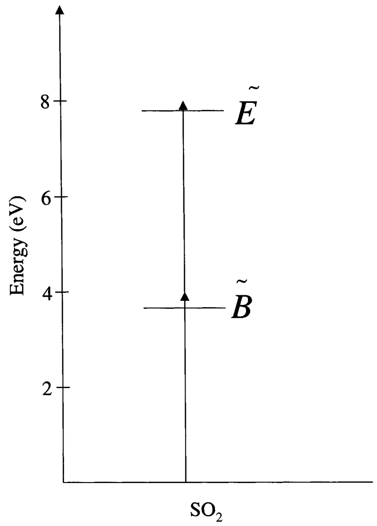

Figure 5. Three individual components comprise the fit displayed in Figure 3. A Gaussian distribution models the experimental pulse width. Rise and decay dynamics of the SO fragment as well as an additional curve corresponding to rise dynamics completes the fitting.

Considering the third proposed mechanism, the pump−probe transient for SO was fit using the kinetics equations convoluted

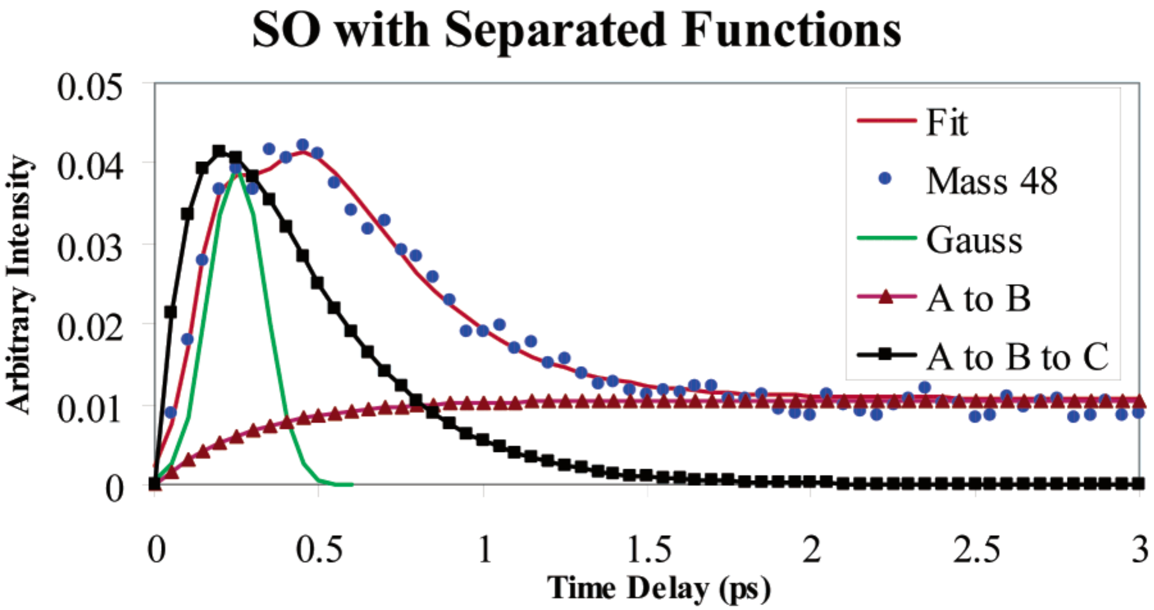

Figure 6. Pump−probe transient for the sulfur fragment. The inset contains the transient of the oxygen cation.

along with the pulse width of the femtosecond laser to yield the production and decay times. The data for the SO fragment was best fit using the following equations to determine kinetic rates:

$$[\mathrm{B}] = \frac{[\mathrm{A}]_0 k_1}{k_2 - k_1}[e^{-k_1 t} - e^{-k_2 t}] \tag{7}$$

$$[\mathrm{B}'] = [\mathrm{A}]_0 - [\mathrm{A}]_0 e^{-k_2 t} \tag{8}$$

In eq 7, A is SO_2, while B is SO (b $^1\Sigma^+$), and C is the undetected SO (X $^3\Sigma^-$). In eq 8, A is SO_2 while B′ models SO (a $^1\Delta$). The value for k_1 was fit to 3.49 ps^{-1} (287 fs) which agrees nicely, within error, to the value calculated from the SO_2 pump−probe transient single-exponential decay. The value for k_2 was determined to be 6.43 ps^{-1} or 156 fs. Figure 6 displays the SO data along with the underlying kinetics that compose the fitting displayed in Figure 3. The data for SO was mathematically fit using a least-squares method with the aid of Microsoft Excel.

The pump−probe transient data for S atomic ion is illustrated in Figure 4; the inset of the figure is the transient for the O atomic ion. Due to the noise level of the data, it is not possible to determine if the data are best fit to kinetics that describe a formation and decay of S, or if the data simply reflect a formation rate with a Gaussian pulse overlap. Both SO and S can radiatively decay from highly excited states if pumped by two additional UV photons. However, this is impossible in these experiments due to the ultrashort nature of the light, the UV pulse is no longer irradiating the molecules after the initial photodissociation and hence, further excitation is not allowed. Furthermore, considering the resolution of the TOF-MS in the present experiments, it is not possible to discern the translational energy obtained by the S photofragments to infer initial excitation energy in these studies as Sato was able to accomplish. As a result of the third proposed mechanism above, the S photofragment is interpreted as a post-ionization fragment of the SO cation.

The SO^+ may fragment after ionization to form either S^+ + O or S + O^+. The relative intensities of O and S do not scale to the ratios present in SO. This is due to the relative ionization potentials (IP) of each of the species; O requires two additional probe photons for ionization. The IPs of various sulfur-containing species and products are given in Table 1. Since the IP of oxygen atom is considerably higher than the others, it is reasonable that fewer of those atoms will arise from the fragmentation of SO^+ and retain the charge to be detected in the mass spectrum. If fragmentation of SO results in S just after photoionization, the sulfur atom would more likely garner the charge from the parent molecule rather than from the oxygen atom. Also, the generation of atomic cation species from SO_2 is low considering the high fluences required for ionization and is only appreciable around the zero overlap.

TABLE 1: Ionization Potentials of the Various Fragments of SO_2

cation	parent	IP (eV)
SO_2^+	SO_2	12.349
SO^+	SO	10.294
S^+	S	10.360
O^+	O	13.618
SO^+	SO_2	15.930
S^+	SO_2	16.334
O^+	O_2	18.690

Conclusions

The decay rate of the SO_2 molecule was calculated to be 271 ± 8 fs. The subsequent formation of SO was produced with the same kinetics and reaffirmed by the fitting procedures utilized. Several independent processes may be occurring in the photodissociation of SO_2; however, the likelihood that they simultaneously occur with the same kinetics is doubtful considering the single-exponential behavior on the SO_2 molecule. Two-photon photodissociation of SO_2 may proceed after excitation to the $\tilde{E}$ state. The production of SO in a higher lying excited state must radiatively decay from the excited state to yield dynamics exhibited in the pump−probe optical transient. A more extensive theoretical approach to SO_2 is necessary to discern the processes studied here. Much theoretical and experimental work has been performed on the lower excited state of SO_2; however, the energetics of two-photon dissociation needs to be explored more completely. Further studies on SO_2 in other excited states are underway to determine the effect of solvation upon the excited-state dynamics and the role they may play in the formation of acid rain.

Acknowledgment. The authors gratefully acknowledge the Department of Energy, Grant No. DE-FG02-92ER14258, for funding this research.

References and Notes

(1) Sander, U. H. F.; Fischer, H.; Rothe, U.; Kola, R. *Sulphur, Sulphur Dioxide and Sulphuric Acid*; Verlag Chemie International Inc.: Deerfield Beach, Fl 1984.

(2) Spiro, P. A.; Jacob, D. J.; Logan, J. A. *J. Phys. Res.* **1992**, *97*, 6023.

(3) Vincent, M. A.; Palmer, I. J.; Miller, I. H.; Akhmatskaya, E. *J. Am. Chem. Soc*. **1998**, *120*, 3431.

(4) Zhong, Q.; Hurley, S.; Castleman, A. W., Jr. *Int. J. Mass Spectrom. Ion Process*. **1999**, *185/186/187*, 905.

(5) Hewitt, C. N. *Atmos. Environ*. **2001**, *35*, 1155.

(6) .Tang, I. N.; Castleman, A. W., Jr. *J. Photochem*. **(1976/77)**, *6*, 349.

(7) .Holland, P. M.; Castleman, A. W., Jr. *J. Photochem*. **1981**, *16*, 347.

(8) Yang, X.; Castleman, A. W., Jr. *Chem. Phys. Lett*. **1991**, *179*, 361.

(9) Yang, X.; Castleman, A. W., Jr. *J. Phys. Chem*. **1991**, *95*, 6182.

(10) Keesee, R. G.; Kilgore, K.; Breen, J. J.; Castleman, A. W., Jr. *Aerosol Sci. Technol*. **1987**, *6*, 71.

(11) Freedman, A.; Yang, S. C.; Bersohn, R. *J. Chem. Phys*. **1979**, *70*, 5313.

(12) Kawasaki, M.; Sato, H. *Chem. Phys. Lett*. **1987**, *139*, 585.

(13) Katagiri, H.; Sako, T.; Hishikawa, A.; Yazaki, T.; Onda, K.; Yamanouchi, K.; Yoshino, K. *J. Mol. Struct*. **1997**, *413/414*, 589.

(14) Lalo, C.; Vermeil, C. *J. Photochem.* **1973**, *1*, 321.

(15) Lalo, C.; Vermeil, C. *J. Photochem.* **1975**, *3*, 441.

(16) Venkitachalam, T.; Bersohn, R. *J. Photochem*. **1984**, *26*, 65.

(17) Effenhauser, C. S.; Felder, P.; Huber, J. R. *Chem. Phys*. **1990**, *142*, 311.

(18) Sato, T.; Kinugawa, T.; Arikawa, T.; Kawasaki, M. *Chem. Phys*. **1992**, *165*, 173.

(19) Wiley, W. C.; McLaren, I. H. *Rev. Sci. Instrum.* **1956**, *26*, 1150.

(20) Fiebig, T.; Chachisvilis, M.; Manger, M.; Zewail, A. H.; Douhal, A.; Garcia-Ochoa, I.; de La Hoz Ayuso, A. *J. Phys. Chem. A* **1999**, *103*, 7419.

(21) Huber, K. P.; Herzberg, G. *Molecular Spectra and Molecular Structure: Constants of Diatomic Molecules*; Van Nostrand Reinhold Company: New York, 1979.